



POST-IMPACT DYNAMICS OF TWO MULTI-BODY SYSTEMS ATTEMPTING DOCKING/BERTHING†

CYRIL XAVIER‡, KIM SUN-WOOK, INGHAM MICHEL, MISRA ARUN and
JAAR GILBERT

Department of Mechanical Engineering, McGill University, Montreal, Canada, H3A 2K6

(Received 21 December 1995)

Abstract—Berthing/docking of two spacecraft systems will become quite routine in future operations. The shuttle will dock with the space station during the latter's construction and operation. Malfunctioning satellites will be serviced by the shuttle or other free flyers. Ideally the rendezvous between the two spacecraft systems should be smooth, but in practice, there is always a velocity differential leading to an impact. Undesirable attitude drift, and structural motion if there are flexible components, will follow this impact. This paper studies the dynamics of two multi-body systems attempting a manipulator assisted docking/berthing considering various impact scenarios.

The equations of motion for the two multi-body systems before and after docking/berthing attempt are obtained using the Lagrangian formulation for individual bodies and then eliminating the constraint forces and moments with the help of the natural orthogonal complement of the velocity constraint matrix. An impact model is developed which can handle impact from fully plastic to fully elastic. Two parameters characterizing the impact—the energy loss parameter and the friction parameter—are introduced. Simulation of the post-impact dynamics shows that the values of these parameters have significant influence on the dynamics. Whether the end-effector is free or locked also influences the dynamics. Response using a control scheme to eliminate the undesirable motion in the fully plastic case (i.e. for successful berthing) is presented. © 1998 Elsevier Science Ltd. All rights reserved

1. INTRODUCTION

Berthing/docking of two spacecraft systems will become quite routine in future space operations. The shuttle will dock with the space station during the latter's construction and operation. Malfunctioning satellites will be serviced by the shuttle or other free flyers. It is quite likely that in many cases the berthing of the spacecraft will take place through a manipulator.

In the ideal case, the chaser should approach the target in such a manner that at the time of berthing, the relative velocity between the chaser berthing mechanism (or end-effector) and the target grapple point should be zero. In practice, however, this is not the case and an impact results. The nature of this impact and subsequent dynamics can vary considerably depending on whether the berthing is successful or there is a rebound; but undesirable attitude drift and structural motion of flexible components are experienced in many cases. The objective of this paper is to consider different impact scenarios and study the post-impact dynamics as-

sociated with manipulator-assisted docking/berthing.

There is a large body of literature related to the dynamics and control of flexible multi-body systems in general and flexible manipulator systems, in particular. A review of that literature is beyond the scope of this paper. Only the studies related to capture dynamics or impact dynamics will be discussed here.

Goldsmith[1] analysed the transverse frictionless impact of a mass on a flexible beam. The analytical approach used, although effective for simple beams, cannot be easily extended to flexible multi-body systems. Chapnik and Heppler[2] considered elastic frictionless impact of a spherical mass on a one-link flexible robotic arm. The rigid body rotational motion of the beam was considered negligible during the time of impact, but not the elastic deflection. Thus the beam could be modelled as a cantilever beam during the impact. The principle of conservation of energy during an elastic impact was combined with momentum considerations to establish the post-impact velocity of the striking mass and the vibrational energy of the beam. The main conclusion of interest from this work is that the elastic deflection caused by impact can be neglected.

Wang and Mason[3] modelled the impact dynamics during robotic operations using a graphical method and assuming that the robots are rigid.

†Paper IAF. 94. A3.023 presented at the 45th International Astronautical Congress, October 9–14, 1994, Jerusalem, Israel.

‡Space Systems Engineering, CAE Electronics Ltd., P.O. Box 1800, St. Laurent, Canada H4L 4X4.

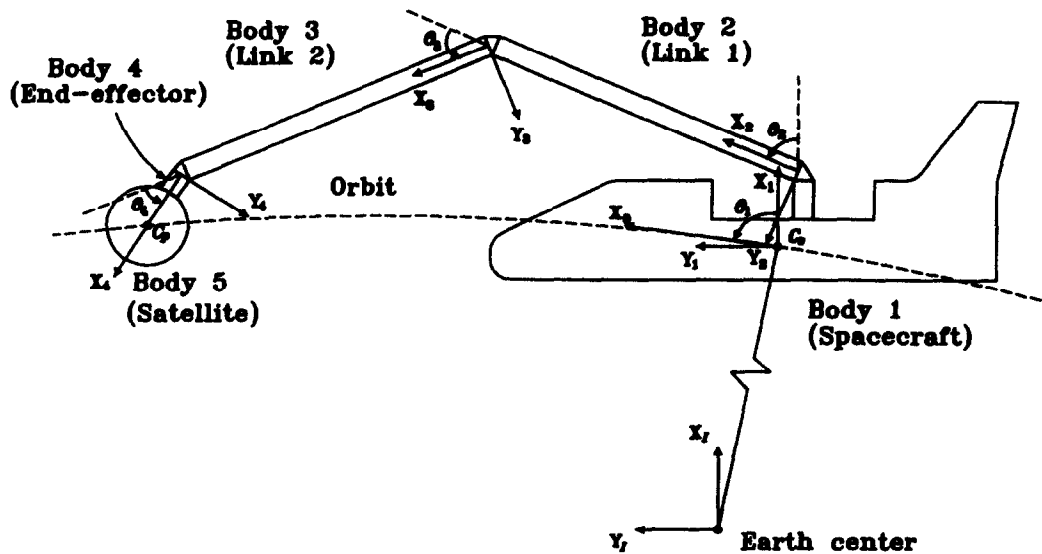


Fig. 1. Schematic diagram of the system under study.

Yoshida *et al.* [4] used the extended generalized inertia tensor (Ex-GIT) and the virtual mass concept to formulate the impact dynamics of a system of free-floating links impacting a point mass in space. The links were modelled as rigid allowing the use of rigid body impact equations for the formulation of a frictionless collision of a fully elastic or a plastic case. The post-impact dynamics, however, was not simulated.

Cyril *et al.* [5] investigated the dynamics of a spacecraft-mounted flexible robotic manipulator capturing a spinning satellite, but the capture was assumed to be smooth. Later, the authors considered cases in which there was a velocity differential between the target grapple point and the end-effector of the flexible manipulator carried by the chaser, and simulated the post-impact dynamics [6]. In all these cases, however, it was assumed that the target was successfully captured, i.e. the impact was fully plastic. The present paper removes this restriction and considers impact scenarios from fully plastic capture to fully elastic rebound.

2. DYNAMICS MODEL

Two orbiting multi-body systems shown in Fig. 1 are considered. Each system has an open chain configuration and may contain one or more flexible bodies. The equations governing the motion of each

of the two systems are obtained using the Lagrangian formulation. Contrary to the usual practice in Lagrangian dynamics where the equations of motions of the system as a whole are derived, the Lagrange equations are derived here for each individual component and then assembled to obtain the equations of motion of the whole system. This approach, however, introduces the non-working generalized forces which are later eliminated by using the natural orthogonal complement of the kinematic velocity constraint matrix [7]. The dynamical equation for each system can then be put in the form

$$\tilde{M}\ddot{\psi} = c(\psi, \dot{\psi}, \psi_0) + f \tag{1}$$

where \tilde{M} is the generalized mass matrix of the system, ψ is the vector of independent generalized coordinates of the system containing both the rigid and elastic degrees of freedom, the vector c contains the velocity dependent inertia terms as well as the damping terms, while f represents the generalized external force vector. The details of the formulation are similar to those in Reference [6] and are omitted here for brevity.

3. IMPACT MODEL

There are two basic assumptions that are made in the formulation of the impact model. The first is

Table 1. Material specification of the 5-body system

Body	length (m)	mass (kg)	EI (N m ²)	I _{zz} (kgm ²)
Spacecraft	N/A	10,000	N/A	40,000
Link 1	8.13	20	8.81×10^2	440.65
Link 2	8.13	20	8.81×10^2	440.65
Hand	0.2	0.2	N/A	2.67×10^{-3}
Payload	N/A	1000	N/A	500

Table 2. Initial conditions of the system

Body	Generalized coordinates (°)	Generalized velocities (° s ⁻¹)
Spacecraft	$\theta_1 = 0$	$\dot{\theta}_1 = 0$
Link 1	$\theta_2 = 67.3$	$\dot{\theta}_2 = 8.36 \times 10^{-1}$
Link 2	$\theta_3 = 45.4$	$\dot{\theta}_3 = -1.81$
Hand	$\theta_4 = 0$	$\dot{\theta}_4 = 9.03 \times 10^{-1}$
Payload	N/A	$\omega = -3.00$

that although the generalized velocities change substantially, the generalized coordinates of the system remain the same over the impact duration. Chapnik and Heppler[2] concluded that this assumption is justified not only for the rotational coordinates but for the elastic coordinates as well. The latter conclusion can also be implied by reasoning that since the duration of impact (approximately 10^{-4} s) is very small compared with the period of the fundamental mode of vibration of the links (several seconds), the change in deflection of a flexible beam during impact is negligible.

The second assumption is that at the contact point between the end-effector and the target there are forces but no moments. In other words, impact occurs at a single point, which is unable to transmit a local moment. This assumption was not made by Cyril *et al.*[6]. If one uses their model, in some cases the moment impulse applied for a plastic impact, $\int_0^t M dt$, is of the order of 10^{-2} N m s. However, the impact duration is usually very short and is of the order of 10^{-4} s. This means that the

average value of the moment is of the order of 10^2 N m (the peak value would be higher). This is a large number for a small end-effector to handle and so it is deemed unrealistic. Accordingly, it is assumed here that there is no impact moment between the end-effector and target.

During collision, the equations of motion of the chaser/manipulator system and the target can be expressed in a form similar to eqn (1), except that in addition to the external forces, there is also the impact load. Thus one can write

$$\tilde{M}\ddot{\Psi} = c + f + J^T f_I \quad (2)$$

$$\tilde{M}_p \ddot{\Psi}_p = c_p + f_p - J_p^T f_I \quad (3)$$

where the subscript p is used for the target, J and J_p are the Jacobians associated with the chaser and target contact points respectively and f_I represents a vector of forces associated with impact. According to the assumption of zero local moment at the impact point, no impact moment terms appear in eqns (2) and (3).

By combining the two eqns of motion (2) and (3), the force vector f_I can be eliminated to yield the following equation:

$$J^T P^{-1} J_p \tilde{M}_p \ddot{\Psi}_p + \tilde{M}\ddot{\Psi} = c + f + J^T P^{-1} J_p (c_p + f_p) \quad (4)$$

where

$$P = J_p J_p^T$$

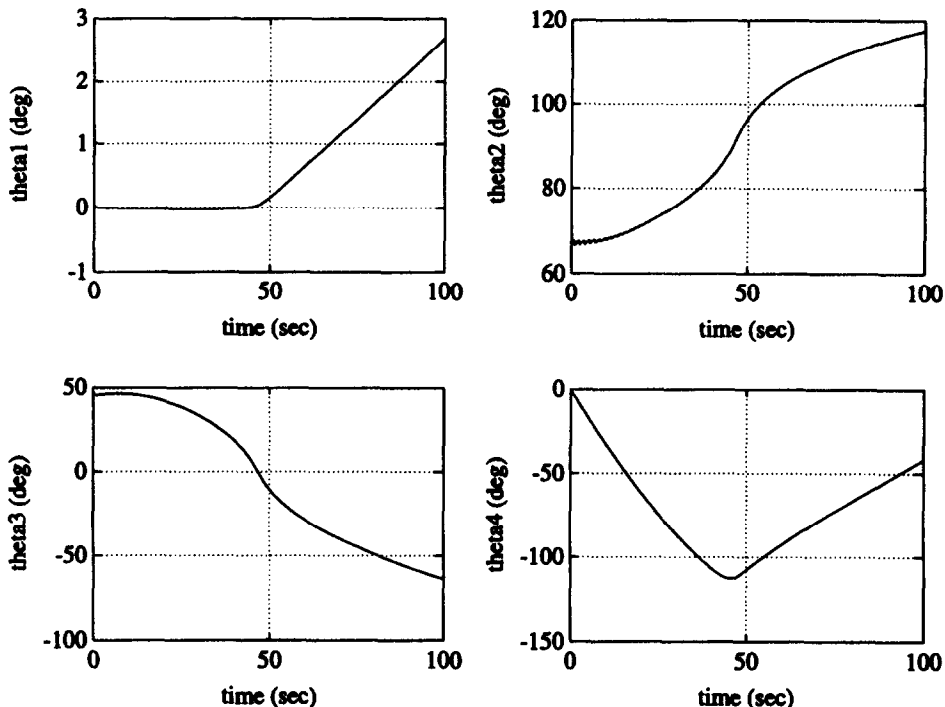


Fig. 2. Spacecraft's pitch and joint angles. Flexible plastic case.

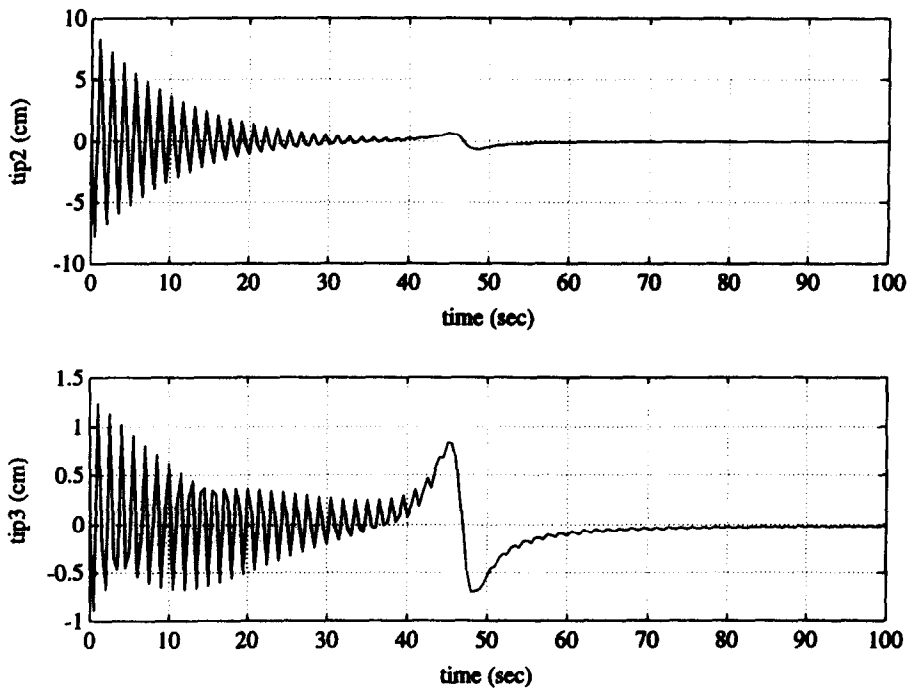


Fig. 3. Link tip deflections. Flexible plastic case.

Note that J_p in general can be a rectangular matrix, which does not have an inverse, but P does.

Now, before integrating the above equation over the period of impact τ , one can recall the assumption that all the generalized coordinates of the sys-

tem remain fixed during this period, although their rates may change. Since J , J_p , \tilde{M}_p and \tilde{M} depend only on the former and not on the latter, these matrices can be taken out of the integral. Also, the impact force is usually very large and acts for a

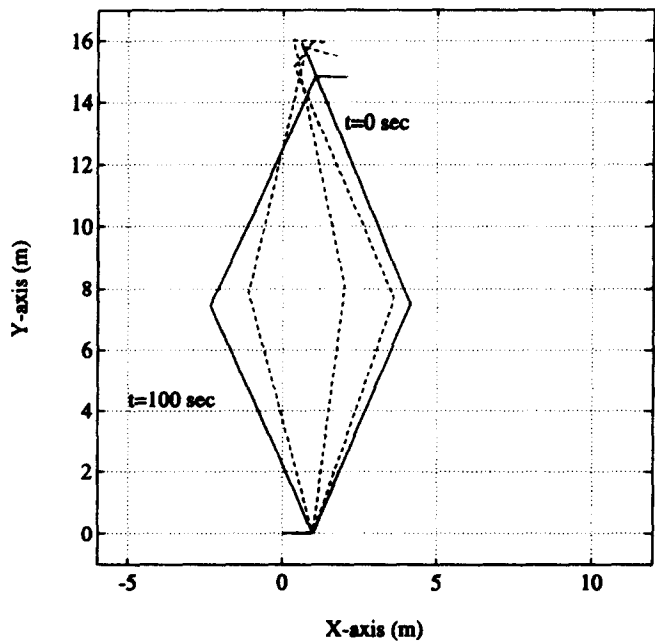


Fig. 4. Configuration of the post-impact system. Flexible plastic case.

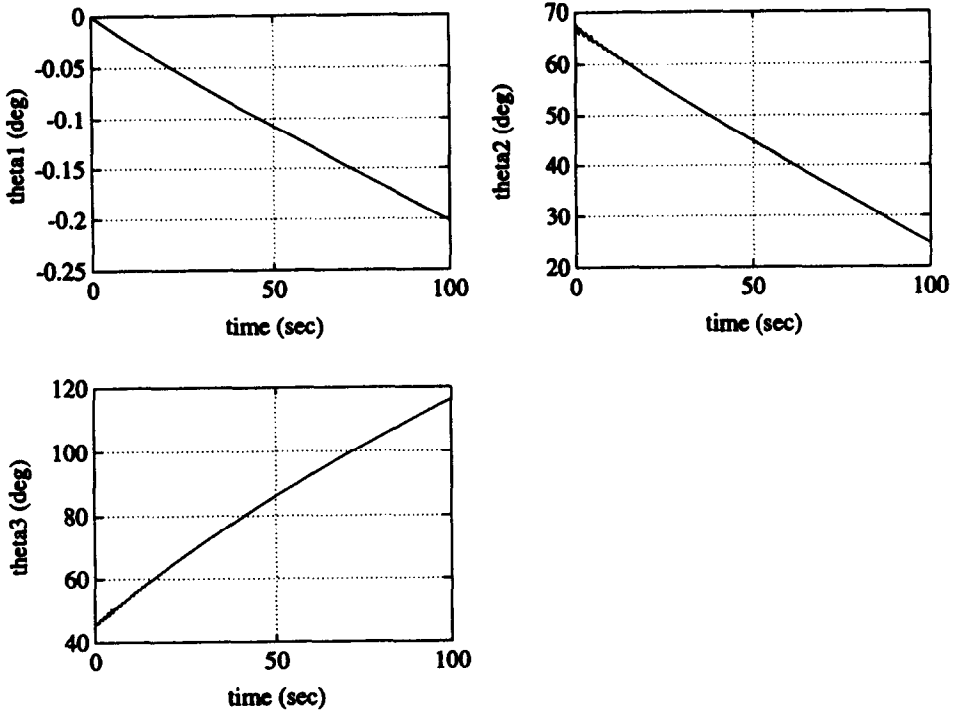


Fig. 5. Spacecraft's pitch and joint angles. Flexible elastic case. Locked end-effector.

very short time τ . Thus, one can say that

$$\tau = \mathcal{O}(\epsilon); \quad \ddot{\psi}, \dot{\psi}_p = \mathcal{O}\left(\frac{1}{\epsilon}\right); \quad \psi, \psi_p, \dot{\psi}, \dot{\psi}_p = \mathcal{O}(1), \quad \epsilon \ll 1 \quad (5)$$

Now, integration of eqn (4) yields

$$\mathbf{J}^T \mathbf{P}^{-1} \mathbf{J}_p \tilde{\mathbf{M}}_p (\dot{\psi}_{pf} - \dot{\psi}_{pi}) + \tilde{\mathbf{M}} (\dot{\psi}_f - \dot{\psi}_i) = \int_0^\tau [\mathbf{c} + \mathbf{f} + \mathbf{J}^T \mathbf{P}^{-1} \mathbf{J}_p (\mathbf{c}_p + \mathbf{f}_p)] dt \quad (6)$$

where the subscripts f and i stand for values after and before the impact. Clearly the left hand side of eqn (6) is $\mathcal{O}(1)$. The integrand on the right hand side is also of $\mathcal{O}(1)$; however, the interval of the integration is of $\mathcal{O}(\epsilon)$ and hence, the right hand side is of $\mathcal{O}(\epsilon)$ and can be ignored compared to the left hand side. Thus eqn (6) becomes

$$\mathbf{J}^T \mathbf{P}^{-1} \mathbf{J}_p \tilde{\mathbf{M}}_p (\dot{\psi}_{pf} - \dot{\psi}_{pi}) + \tilde{\mathbf{M}} (\dot{\psi}_f - \dot{\psi}_i) = 0 \quad (7)$$

Equation (7) is applicable to all collisions ranging from plastic to perfectly elastic. In the case of plastic impact, the two systems become rigidly attached to each other at the contact points after impact, while in the case of elastic impact, the systems rebound with no loss of energy. The former case corresponds to successful capture or berthing.

3.1. Plastic impact

In plastic impact, the velocity of the contact point of each system is the same immediately after the impact. Thus, one obtains

$$\mathbf{J} \dot{\psi}_f = \mathbf{J}_p \dot{\psi}_{pf} \quad (8)$$

One can then solve for the generalized velocities of the target in terms of those of the chaser to obtain

$$\dot{\psi}_{pf} = \mathbf{Q}^{-1} \mathbf{J}_p^T \mathbf{J} \dot{\psi}_f \quad (9)$$

where

$$\mathbf{Q} = \mathbf{J}_p^T \mathbf{J}_p$$

Substitution of eqn (9) into (7) yields

$$\dot{\psi}_f = \mathbf{G}^{-1} \mathbf{H} \quad (10)$$

where

$$\mathbf{G} = \mathbf{J}^T \mathbf{P}^{-1} \mathbf{J}_p \tilde{\mathbf{M}}_p \mathbf{Q}^{-1} \mathbf{J}_p^T \mathbf{J} + \tilde{\mathbf{M}} \quad (11)$$

$$\mathbf{H} = \mathbf{J}^T \mathbf{P}^{-1} \mathbf{J}_p \tilde{\mathbf{M}}_p \dot{\psi}_{pi} + \tilde{\mathbf{M}} \dot{\psi}_i \quad (12)$$

Once $\dot{\psi}_f$ for the chaser has been determined, one can use eqn (9) to evaluate $\dot{\psi}_{pf}$ for the target (or payload). Equations (9) and (10) hold good for any two flexible multi-body systems undergoing a plastic impact and can be used as long as \mathbf{P} and \mathbf{Q} are non-singular.

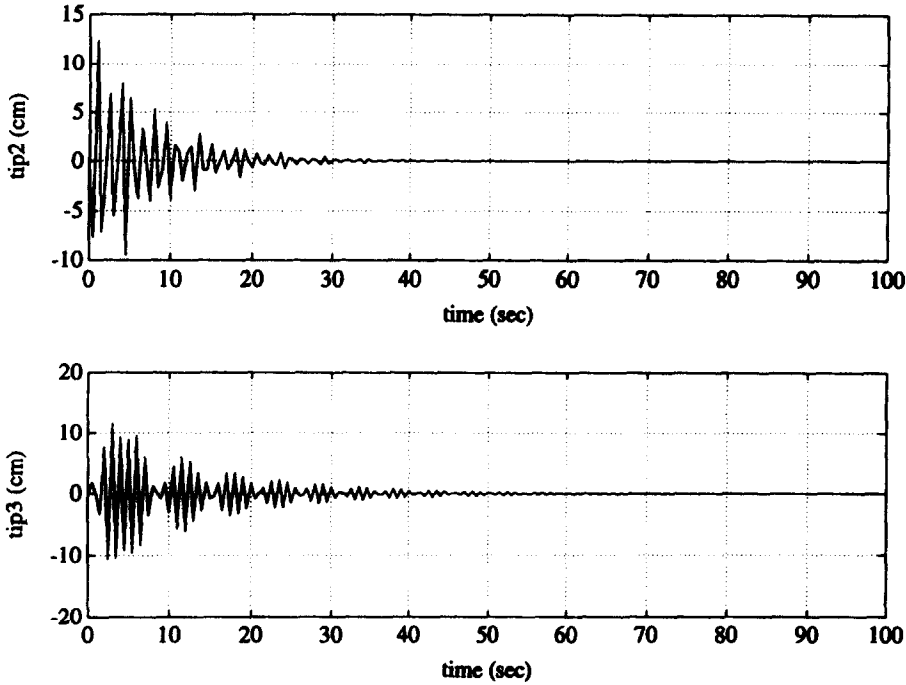


Fig. 6. Link tip deflections. Flexible elastic case. Locked end-effector.

A special case of interest is when one of the systems is a rigid body. This situation occurs when the shuttle/manipulator system captures a disabled, basically rigid satellite or when the space station/manipulator system docks with the shuttle. From the post-impact dynamics simulation point of view, it is immaterial as to which system has an active trajectory control. For our analysis, the rigid body is termed the target (or the payload).

If the payload is a single rigid body, eqn (3) can be written as

$$\mathbf{M}_p \dot{\mathbf{w}}_p = \mathbf{f}_p - \mathbf{A} \xi_1 \quad (13)$$

where \mathbf{w}_p is the 6-dimensional velocity vector consisting of the velocity of the center of mass and the angular velocity components, \mathbf{M}_p is the extended mass matrix which can be written as

$$\mathbf{M}_p = \begin{bmatrix} m_p \mathbf{I} & 0 \\ 0 & \mathbf{I}_p \end{bmatrix} \quad (14)$$

where m_p is the mass of the payload, \mathbf{I} is the 3×3 unit matrix and \mathbf{I}_p is the centroidal inertia matrix, while ξ_1 is a 6×1 vector consisting of \mathbf{f}_1 appearing in eqns (2) and (3) and a 3×1 zero vector. Furthermore, \mathbf{A} can be expressed as

$$\mathbf{A} = \begin{bmatrix} \mathbf{I} & 0 \\ \mathbf{R}_{pb} & \mathbf{I} \end{bmatrix} \quad (15)$$

where \mathbf{I} is the 3×3 unit matrix and \mathbf{R}_{pb} is the cross-product tensor of \mathbf{r}_{pb} , which is the position vector of the payload's contact point with respect to its centre of mass.

The post-impact generalized velocity vector $\dot{\psi}_f$ of the chaser or the manipulator-carrying spacecraft is again given by eqn (10), except that \mathbf{G} and \mathbf{H} now have the following forms:

$$\mathbf{G} = m_p \mathbf{J}^T \mathbf{K}^{-1} \mathbf{J} + \tilde{\mathbf{M}} \quad (16)$$

$$\mathbf{H} = -m_p \mathbf{J}^T [\mathbf{K}^{-1} (-m_p \mathbf{R}_{pb} \mathbf{I}_p^{-1} \mathbf{R}_{pb} \mathbf{v}_{pi} + \mathbf{R}_{pb} \boldsymbol{\omega}_{pi}) - \mathbf{v}_{pi}] + \tilde{\mathbf{M}} \dot{\psi}_i \quad (17)$$

where

$$\mathbf{K} = \mathbf{I} - m_p \mathbf{R}_{pb} \mathbf{I}_p^{-1} \mathbf{R}_{pb} \quad (18)$$

The velocity of the centre of mass of the rigid body and its angular velocity just after the impact are given by

$$\mathbf{v}_{pf} = \mathbf{K}^{-1} (\mathbf{J} \dot{\psi}_f - m_p \mathbf{R}_{pb} \mathbf{I}_p^{-1} \mathbf{R}_{pb} \mathbf{v}_{pi} + \mathbf{R}_{pb} \boldsymbol{\omega}_{pi}) \quad (19)$$

$$\boldsymbol{\omega}_{pf} = m_p \mathbf{I}_p^{-1} \mathbf{R}_{pb} (\mathbf{v}_{pf} - \mathbf{v}_{pi}) + \boldsymbol{\omega}_{pi} \quad (20)$$

Hence, from the pre-impact conditions, $\dot{\psi}_f$ can be calculated using eqns (10) and (16)–(18) after which \mathbf{v}_{pf} and $\boldsymbol{\omega}_{pf}$ can be calculated, in that order, using eqns (19) and (20).

3.2. Non-plastic impact

If the impact is perfectly elastic, there is no energy loss during the impact. Fully elastic and fully plastic impact are the two extreme cases; a general non-plastic case lies between these two. In the present formulation, two parameters are used to

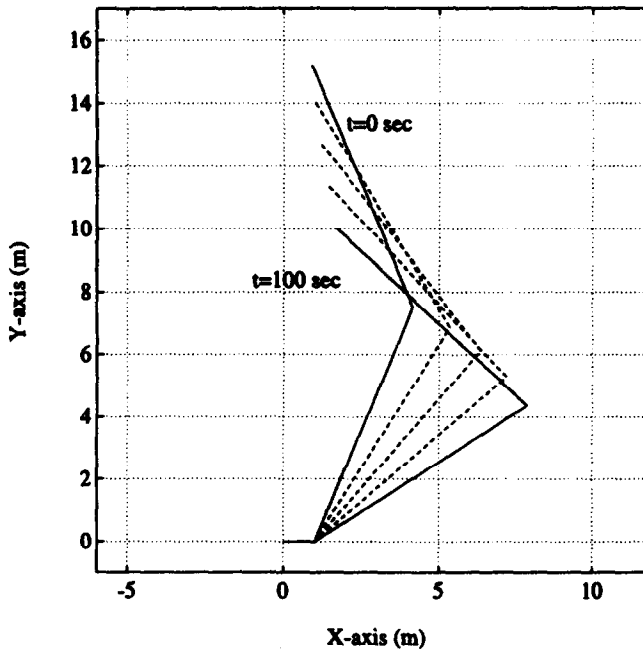


Fig. 7. Configuration of the post-impact system. Flexible elastic case. Locked end-effector.

characterize the impact—they are the energy loss parameter r_E and the friction parameter r_f , which represents fractions of the loss of kinetic energy and friction impulse, respectively, of the plastic case. That is,

$$r_E = \frac{|\Delta KE|_{(\text{particular case})}}{|\Delta KE|_{(\text{plastic case})}} \quad (21)$$

$$r_f = \frac{P_{(\text{particular case})}}{P_{(\text{plastic case})}} \quad (22)$$

Therefore,

- $r_E=1$ corresponds to the kinetic energy loss which occurs in a plastic impact.
- $r_E=0$ corresponds to no kinetic energy loss which occurs in an elastic impact.
- $r_f=1$ corresponds to the friction impulse $\int_0^t f_f dt$ in a plastic impact.
- $r_f=0$ corresponds to no friction force which is the case in an elastic impact because friction involves energy losses and an elastic impact is by definition a case in which there is no energy loss.

It may sometimes be possible that for two specified parametric values of friction and loss of kinetic energy a real solution will not be found. For example, if $r_f=0$ and $r_E=1$ were specified, no solution will be found which satisfies the equations of impact because friction is needed to make a partial contribution to the energy loss and the values of the two parameters are inconsistent. In other words, r_E and r_f must be selected judiciously if they

are to represent a physically plausible impact problem.

Let us now express the above statements in mathematical form. To keep the analysis simple, the target will be assumed to be a rigid body although the chaser is a flexible multi-body system.

Since the problem of a plastic impact has already been solved in Section 3.1, the friction impulse during this impact can be calculated as follows:

$$P_{t,p} = -m_p(v_{ptf} - v_{pti}) \quad (23)$$

where

$$v_{ptf} = (v_{pf} \cdot t)t \quad (24)$$

$$v_{pti} = (v_{pi} \cdot t)t \quad (25)$$

p_t stands for the impulse vector due to friction, and t is a unit vector along the direction of the friction force. This vector can be found by using the following relation:

$$t = \frac{v_{hi} - (v_{hi} \cdot n)n - [v_{bi} - (v_{bi} \cdot n)n]}{|v_{hi} - (v_{hi} \cdot n)n - [v_{bi} - (v_{bi} \cdot n)n]|} \quad (26)$$

where the subscripts h and b stand for contact points of the main system and payload, respectively.

Similarly, the kinetic energy loss during the plastic impact can be expressed as:

$$\Delta KE_p = \frac{1}{2} [\dot{\psi}_f^T \tilde{M} \dot{\psi}_f + w_f^T M_p w_f - \dot{\psi}_i^T \tilde{M} \dot{\psi}_i - w_i^T M_p w_i] \quad (27)$$

where the subscript f here stands for the final values in the plastic impact.

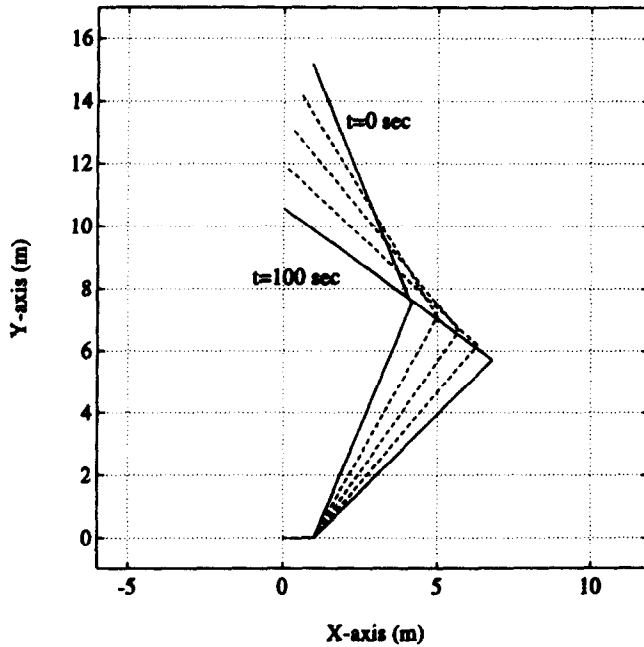


Fig. 8. Configuration of the post-impact system. Flexible. $r_E=0.5$, $r_f=0.5$. Locked end-effector.

Considering only the payload, the velocity has three components namely, v_{pn} , v_{pt} and v_{pm} , where \mathbf{n} is a unit vector along the line of impact and directed from the payload to the end-effector, \mathbf{t} is as defined earlier, and $\mathbf{m} = \mathbf{nxt}$.

Defining,

$$v_{pni} = x\mathbf{n} \text{ and } v_{pnf} = -e\mathbf{n} \quad (28)$$

the velocity before and after impact can be expressed as:

$$v_{pi} = x\mathbf{n} + v_{pti} + v_{pmi} \quad (29)$$

$$v_{pf} = -e\mathbf{n} + v_{ptf} + v_{pmi} \quad (30)$$

where it should be noticed that the velocity component v_{pm} is the same before and after impact.

The velocity change in the \mathbf{t} direction is only due to the friction impulse. Therefore,

$$v_{ptf} = -\frac{r_f \mathbf{p}_{t,p}}{m_p} + v_{pti} \quad (31)$$

The change in velocity of the payload's center of mass may now be expressed as follows:

$$v_{pf} - v_{pi} = -(e+x)\mathbf{n} - \frac{r_p \mathbf{p}_{t,p}}{m_p} \quad (32)$$

Now, integrating eqn (13) and noting that there is no local impulse moment at the contact point, one obtains

$$-m_p \mathbf{R}_{pb}(v_{pf} - v_{pi}) + \mathbf{I}_p(\omega_{pf} - \omega_{pi}) = \mathbf{0}_{3 \times 1} \quad (33)$$

From eqn (33), the final angular velocity may be isolated as:

$$\begin{aligned} \omega_{pf} &= m_p \mathbf{I}_p^{-1} \mathbf{R}_{pb}(v_{pf} - v_{pi}) + \omega_{pi} \\ &= m_p \mathbf{I}_p^{-1} \mathbf{R}_{pb} \left[-(e+x)\mathbf{n} - \frac{r_f \mathbf{p}_{t,p}}{m_p} \right] + \omega_{pi} \end{aligned} \quad (34)$$

Now, defining,

$$e^* = m_p(e+x) \quad (35)$$

$$\mathbf{s} = \mathbf{I}_p^{-1} \mathbf{R}_{pb} \mathbf{n} \quad (36)$$

and

$$\mathbf{z} = -r_f \mathbf{I}_p^{-1} \mathbf{R}_{pb} \mathbf{p}_{t,p} + \omega_{pi} \quad (37)$$

eqn (34) can be written as:

$$\omega_{pf} = -e^* \mathbf{s} + \mathbf{z} \quad (38)$$

When the payload is rigid, eqn (7) for the general case becomes

$$m_p \mathbf{J}^T(v_{pf} - v_{pi}) + \tilde{\mathbf{M}}(\dot{\psi}_f - \dot{\psi}_i) = \mathbf{0} \quad (39)$$

From eqns (32) and (39), one obtains

$$\dot{\psi}_f = e^* \tilde{\mathbf{M}}^{-1} \mathbf{J}^T \mathbf{n} + r_f \tilde{\mathbf{M}}^{-1} \mathbf{J}^T \mathbf{p}_{t,p} + \dot{\psi}_i \quad (40)$$

Defining,

$$\mathbf{u} = \tilde{\mathbf{M}}^{-1} \mathbf{J}^T \mathbf{n} \quad (41)$$

$$\mathbf{u}^* = r_f \tilde{\mathbf{M}}^{-1} \mathbf{J}^T \mathbf{p}_{t,p} + \dot{\psi}_i \quad (42)$$

eqn (40) can be re-written as follows:

$$\dot{\psi}_f = e^* \mathbf{u} + \mathbf{u}^* \quad (43)$$

Since it is assumed that the generalized coordinates

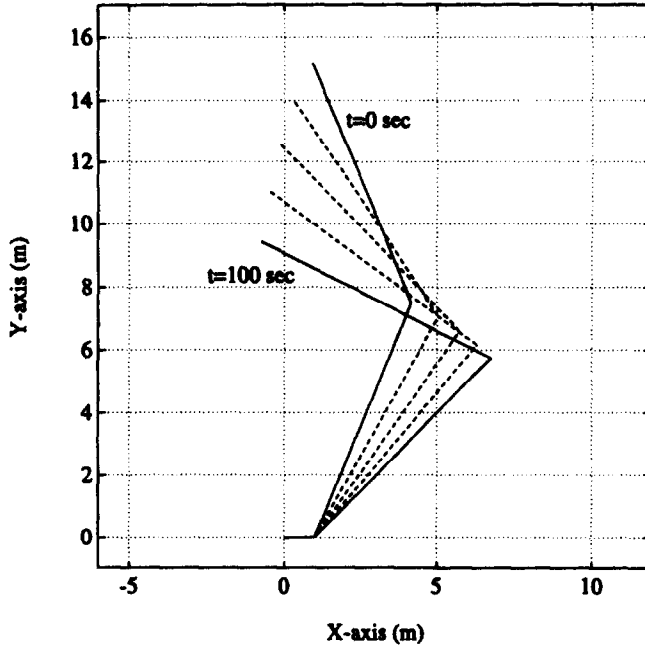


Fig. 9. Configuration of the post-impact system. Flexible. $r_E=0.5$, $r_f=0.8$. Locked end-effector.

of the system do not change during impact, the change in potential energy is negligible and only kinetic energy accounts for the change in mechanical energy.

Let r represent the ratio of initial to final kinetic energy as follows:

$$r = \frac{\frac{1}{2} \mathbf{w}_{pf}^T \mathbf{M}_p \mathbf{w}_{pf} + \frac{1}{2} \dot{\Psi}_f^T \tilde{\mathbf{M}} \dot{\Psi}_f}{\frac{1}{2} \mathbf{w}_{pi}^T \mathbf{M}_p \mathbf{w}_{pi} + \frac{1}{2} \dot{\Psi}_i^T \tilde{\mathbf{M}} \dot{\Psi}_i} \quad (44)$$

The ratio r can be found from the kinetic energy loss parameter r_E by the following relation:

$$r = \frac{KE_i - r_E |\Delta KE_p|}{KE_i} \quad (45)$$

where KE_i is the initial kinetic energy of the system.

The term $\mathbf{w}_p^T \mathbf{M}_p \mathbf{w}_p$ can be decomposed as:

$$\mathbf{w}_p^T \mathbf{M}_p \mathbf{w}_p = m_p \mathbf{v}_p^T \mathbf{v}_p + \boldsymbol{\omega}_p^T \mathbf{I}_p \boldsymbol{\omega}_p \quad (46)$$

Therefore, we can write:

$$\begin{aligned} \mathbf{w}_{pf}^T \mathbf{M}_p \mathbf{w}_{pf} &= m_p (e^2 \mathbf{n}^T \mathbf{n} - 2e \mathbf{n}^T \mathbf{v}'_{pf} + \mathbf{v}'_{pf} \mathbf{v}'_{pf}) \\ &\quad + e^2 \mathbf{s}^T \mathbf{I}_p \mathbf{s} - 2e^* \mathbf{I}_p \mathbf{z} + \mathbf{z}^T \mathbf{I}_p \mathbf{z} \end{aligned} \quad (47)$$

where $\mathbf{v}'_{pf} = \mathbf{v}_{ptf} + \mathbf{v}_{pmf}$.

Also,

$$\dot{\Psi}_f^T \tilde{\mathbf{M}} \dot{\Psi}_f = e^{*2} \mathbf{u}^T \tilde{\mathbf{M}} \mathbf{u} + 2e^* \mathbf{u}^T \tilde{\mathbf{M}} \mathbf{u}^* + \mathbf{u}^{*T} \tilde{\mathbf{M}} \mathbf{u}^* \quad (48)$$

Substituting these decomposed terms into eqn (44) we get the following relation:

$$pe^2 + qe + r^* = 0 \quad (49)$$

where

$$p = m_p \mathbf{n}^T \mathbf{n} + m_p^2 \mathbf{s}^T \mathbf{I}_p \mathbf{s} + m_p^2 \mathbf{u}^T \tilde{\mathbf{M}} \mathbf{u}$$

$$\begin{aligned} q &= 2(-m_p \mathbf{n}^T \mathbf{v}'_{pf} + m_p^2 \mathbf{x}^T \mathbf{I}_p \mathbf{s} - m_p \mathbf{s}^T \mathbf{I}_p \mathbf{z} \\ &\quad + m_p^2 \mathbf{x} \mathbf{u}^T \tilde{\mathbf{M}} \mathbf{u} + m_p \mathbf{u}^T \tilde{\mathbf{M}} \mathbf{u}^*) \end{aligned}$$

$$\begin{aligned} r^* &= m_p \mathbf{v}_{pf}^T \mathbf{v}'_{pf} + m_p^2 \mathbf{x}^2 \mathbf{s}^T \mathbf{I}_p \mathbf{s} - 2m_p \mathbf{x} \mathbf{s}^T \mathbf{I}_p \mathbf{z} \\ &\quad + \mathbf{z}^T \mathbf{I}_p \mathbf{z} + m_p^2 \mathbf{u}^T \tilde{\mathbf{M}} \mathbf{u} + 2m_p \mathbf{x} \mathbf{u}^T \tilde{\mathbf{M}} \mathbf{u}^* \\ &\quad + \mathbf{u}^{*T} \tilde{\mathbf{M}} \mathbf{u}^* - r(\mathbf{w}_{pi}^T \mathbf{M}_p \mathbf{w}_{pi} + \dot{\Psi}_i^T \tilde{\mathbf{M}} \dot{\Psi}_i) \end{aligned}$$

The values of 'e' are found from eqn (49), from which depending on the initial conditions of the system, the correct 'e' must be chosen. Here are some of its characteristics.

Depending on the direction of the payload's initial velocity component \mathbf{v}_{ni} , 'e' satisfies the following conditions:

$$\text{if } x \geq 0 \text{ then } \mathbf{v}_{nf} - \mathbf{v}_{ni} \leq 0 \text{ or } e + x \geq 0 \quad (50)$$

$$\text{if } x < 0 \text{ then } \mathbf{v}_{nf} - \mathbf{v}_{ni} > 0 \text{ or } e + x < 0 \quad (51)$$

Another characteristic of 'e' is that for any type of impact scenario, the larger the kinetic energy loss or the smaller the friction impulse, the smaller will be the effect of impact on the final value of the velocity component of the payload, \mathbf{v}_{pnf} , that is,

$$|e + x|_{r_E} > |e + x|_{r_f} \quad (52)$$

$$|e + x|_{r_f} < |e + x|_{r_f^*} \quad (53)$$

where r_E^* and r_f^* are larger than r_E and r_f , respectively.

The right value of ' e ' must be chosen from the two roots of eqn (49) such that it satisfies the above characteristics. This value is in turn substituted into eqns (35), (32), (38) and (43) in order to find e^* , the final linear and the angular velocity of the payload and the final generalized velocity vector of the manipulator/spacecraft system, respectively.

These final values of \mathbf{w}_{pf} and ψ_f are used as initial conditions for the post-impact dynamical eqns of the system, which includes the payload if impact is plastic, and does not if it is non-plastic.

4. SIMULATION RESULTS AND DISCUSSION

In order to compare various impacts, a spacecraft-manipulator system impacting on a rigid payload is considered. The system parameters are given in Table 1. The non-zero initial conditions are given in Table 2. All others have zero initial conditions. Figures 2 and 3 show the post-impact dynamics for the plastic impact case. Corresponding configuration variation is shown in Fig. 4. Corresponding dynamics for the fully elastic case of rebound is shown in Figs 5–7, respectively. A comparison of Figs 4 and 7 shows that there is a significant difference in the post-impact motion between the fully plastic and the fully elastic cases. In the plastic case, the payload has a large angular momentum which tends to stretch out the manipulator arms until the singularity configuration, at which point a moment is induced in both the payload and the base of the

spacecraft, which causes the former to change its direction of rotation and the latter to experience attitude drift. For a non-plastic case, the motion is simpler. The manipulator is a small mass which stretches out to hit against a large mass (payload) and simply rebounds as it tends to fold back on itself.

For non-plastic impact, there are differences to be observed depending on the values of the two parameters, friction and energy-loss:

- (i) *friction parameter*; as described before, the impulse that is involved in the collision at the contact point can be divided into two components: one is along the line of impact (normal impulse), and the other is perpendicular to it (friction impulse). If the friction impulse exists, the resultant impact force is the vector summation of these two components and so, as seen by comparing Fig. 8 ($r_E=0.5$, $r_f=0.5$) and Fig. 9 ($r_E=0.5$, $r_f=0.8$), the post-impact motion of the system is influenced by this change in direction and magnitude of the resultant impulse (compare the X - Y positions of the manipulator tip).
- (ii) *energy-loss parameter*; for a fixed friction parameter, the energy-loss parameter influences the normal impulse so that this parameter also is seen to change the direction and magnitude of the resultant impulse. It is also possible to interpret this parameter purely in terms of energy: for example, if the kinetic energy loss of the system (including satellite) is small, the manipulator system usually has more initial kinetic energy and so its tip moves further as seen in

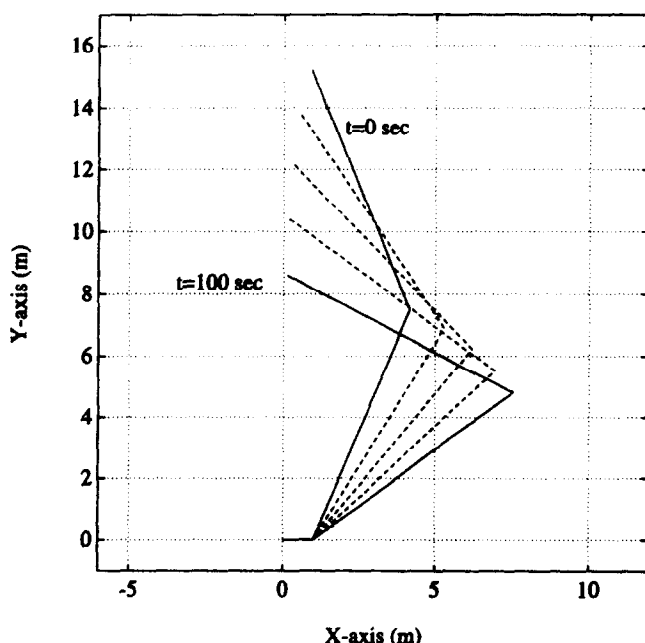


Fig. 10. Configuration of the post-impact system. Flexible. $r_E=0.2$, $r_f=0.5$. Locked end-effector.

Fig. 10 ($r_E=0.2$, $r_f=0.5$) as compared to Fig. 8 ($r_E=0.5$, $r_f=0.5$).

5. CONCLUDING REMARKS

A methodology for formulating the impact dynamics during the berthing/capture process was presented. Two multi-body flexible systems were considered for the plastic impact (successful capture) case, but for the non-plastic case one of the systems was a rigid body. Using the impact model, a set of post-impact values of the generalized velocities of the system are determined, which are used as initial conditions for the post-impact dynamic simulation of the system.

It was found that it is important to model the flexibility of the links if accurate results are to be obtained in the post-impact dynamic simulation, especially for non-plastic cases. It was also noticed that plastic impact leads to significantly different dynamics from non-plastic impact. Two parameters characterizing an impact were introduced: the energy loss parameter r_E and the friction parameter r_f . It was found that depending on the values of the two impact parameters, the resultant impact impulse changes direction and magnitude, which in

turn has a significant effect on the motion of the manipulator system.

Acknowledgements—The authors wish to express their gratitude to the Natural Sciences and Engineering Research Council of Canada (NSERC) for providing the funding for this research.

REFERENCES

1. Goldsmith, W., *Impact*, London: Edward Arnold Ltd, 1960.
2. Chapnik, B. V., Heppler, G. R. and Aplevich, J. D., *IEEE Transactions on Robotics and Automation*, 1991, 7, 479–488.
3. Wang, Y. and Mason, M., in *Proceedings of the 1987 IEEE International Conference on Robotics and Automation*, 2, 1987, pp. 686–695.
4. Yoshida, K., Kurazume, R., Sashida, N. and Umetani, Y., Modeling of collision dynamics for space free-floating links with extended generalized inertia tensor, in *Proceedings of the 1992 IEEE Conference on Robotics and Automation*, Nice, France, May, 1992.
5. Jaar, G. J., Cyril, X. and Misra, A. K., *Acta Astronautica*, 1995, 35, 167–174.
6. Cyril, X., Jaar, G. J., Ingham, M. and Misra, A. K., Post-impact dynamics of a spacecraft-mounted manipulator, *44th Congress of the International Astronautical Federation*, Graz, Austria, October, 1993, pp. 16–22.
7. Cyril, X., Angeles, J. and Misra, A. K., Dynamics of flexible multibody mechanical systems, *Transactions of the CSME*, 15(3), 1991.